

Measurements of $^{nat}Pb(p, xn)^{201-207}Bi$, $^{204}Pb(p, 1 - 4n)^{201-204}Bi$ and $^{206}Pb(p, 3n)^{204}Bi$ cross-sections at astrophysical energies ($E_p \leq 30 MeV$)

P.V. Guillaumon,* I.D. Goldman, and V.R. Vanin
*Universidade de Sao Paulo Instituto de Fisica
Rua do Mato 1371, 05508-090 Sao Paulo, Brazil*

H. Barcellos de Oliveira
*Instituto de Pesquisas Energticas e Nucleares/Comisso Nacional de Energia Nuclear
Av. Prof. Lineu Prestes, 2242, 05508-000 Sao Paulo, Brazil*
(Dated: March 5, 2022)

Cross-sections for $^{nat}Pb(p, xn)^{201-207}Bi$, $^{204}Pb(p, 1 - 4n)^{201-204}Bi$ and $^{206}Pb(p, 3n)^{204}Bi$ reactions have been determined in the astrophysical energy range 20 – 30 MeV. The analysis were performed by γ -spectroscopy associated with half-lives measurements. The results were compared with previously experimental data, when available, and with theoretical calculations performed using TALYS code. We report a possible new γ transition from ^{204m}Pb and other theoretical discrepancies, probably due overestimation of the Coulomb barrier and neutron binding energy. Also reported are new determinations of the energies and intensities of the γ 's emitted in the decays of $^{205,206}Bi$. We discuss possible implications for the r/rp-processes in neutrino-driven wind in supernovae and neutron stars mergers.

I. INTRODUCTION

The rp-process is not fully understood in part due lack of experimental data in the proton-rich region. There are several p-only elements like ^{196}Hg , ^{190}Pt , ^{184}Os , and ^{180}W , all near $Z \sim 83$. If an rp-process is responsible for the nucleosynthesis of these isotopes, all the others nearby may be affected too, and could act as poisons of the protons' flux. These nuclear constraints are important for astrophysical models of supernovae and neutron mergers, where this process should takes place.

If the local temperature under supernovae collapse reaches $T > 3 \times 10^9 K$ followed by a proton “freeze-out”, (p, xn) reactions would be important and could enrich p-elements abundances. There are discrepancies on nuclear structure and cross-sections values for neutron deficient heavy elements. Also, there are no measured cross-sections on $^{204}Pb(p, xn)$ reactions on the threshold, neither for $^{nat}Pb(p, xn)^{207}Bi$. The same holds for a bunch of other nuclei in the lead region.

Precise measurements are important as constraints for nuclear-structure calculations and phenomenological models, specially in a region that is not well established yet, and could help to predict properties of other p-nuclides whose cross-sections are almost unknown. Despite its astrophysical importance, there is limited data available, the majority of them performed more than 40 years ago.

The measurement of (p, xn) reactions could have other applications too: the discovery of new viable paths for radio-pharmaceutical isotopes' production. For example, the important ^{201}Tl radionuclide, whose production is, in general, made by $^{203}Tl(p, 2n)^{201}Pb$, could also be

produced by the $^{204}Pb(p, 3n)^{201}Pb$ route.

For ultra-low background measurements like those used in dark matter experiments, high energy cosmic rays could penetrate the shield, after losing energy, and provoke (p, xn) and (p, γ) reactions. Although not likely probable, could be enough to increase the noise.

II. EXPERIMENTAL DETAILS

The samples for these experiments consisted of natural Pb metal foils of $< 0.5 mm$ thickness and 10 mm diameter ($> 99.9\%$ pure). Samples were irradiated at IPEN/CNEN-SP cyclotron facility with protons from 18 to 30 MeV and beam current of a few μA . Since this cyclotron operates only with liquid targets, an adapter to solid ones was made and attached to the target holder.

Gamma spectroscopy with an HPGe detector was performed immediately after irradiation. The samples were measured continuously and the spectra were saved every 30 min, allowing us to follow half-lives from 57.5 min (^{201m}Bi) to 31.55 y (^{207}Bi). The detector resolution at 1332 keV was 2 keV and was coupled to a digital signal processor-based data acquisition system. Energy calibration was done with a second degree polynomial fit based on a weighted non-linear principal component analysis, [1]. The peaks were fitted to Gaussian shapes with tail and linear background using IDEFIX software, [2]. Self-absorption of protons and γ were estimated to be minimal and were not taken into account. The detector was shielded with $\sim 10 cm$ lead, leading to a contribution for the peaks of less than 0.02 Bq.

End-of-bombardment activities ranged from 20 to 40 kBq with a dead-time up to 70% at 20 cm from the detector and were corrected by a $\Delta_{real}/\Delta_{live}$ term, where Δ_{live} is the live time and Δ_{real} , the real one. The cross-section will be given by

* guillaumon@if.usp.br

$$\sigma = \frac{\mathcal{A}e^{\lambda\Delta t}}{\mathcal{N}_0\Phi\varepsilon I_\gamma (1 - e^{-\lambda t_{irr}})} \frac{\Delta t}{\Delta t_{live}}, \quad (1)$$

where \mathcal{A} is the activity of the isotope, λ the decay constant, \mathcal{N}_0 the number of isotopes before irradiation, ε the total efficiency, I_γ the intensity of the γ rays, t_{irr} the time interval between irradiation and measurement, Δt the real time of measurement, and Δt_{live} the live time.

III. RESULTS

Figures 1 and 2 show the γ spectra from the irradiation of ^{nat}Pb with protons of 30 MeV accumulated for about 20 min after irradiation with a live time of

30 min. No appreciable impurities were observed and could be neglected. Several $^{201-207}Bi$ lines lies close to each other with an energy difference of less than 0.5 keV. In principle, we could easily separate them by a careful measurement of the half-lives, since they range from less than one hour to a few ten years. The only exception are the lines of ^{203}Bi (11.76 h) with ^{204}Bi (11.22 h), like the 421.8 keV line (0.39%) of the first one, and the 421.61 keV line (1.14%) of the second. To calculate reactions cross-sections it is preferably to use less intense pure lines than mixed intense ones. We used this criteria, whenever possible. The ^{201}Bi was the only exception, where there were no pure lines.

Detector efficiency and counting statistics were the dominant contribution to the uncertainty, of less than 10% together. Proton flux, sample mass, energy resolution, half-life and β decay branching contribute with less than 5% of the uncertainty.

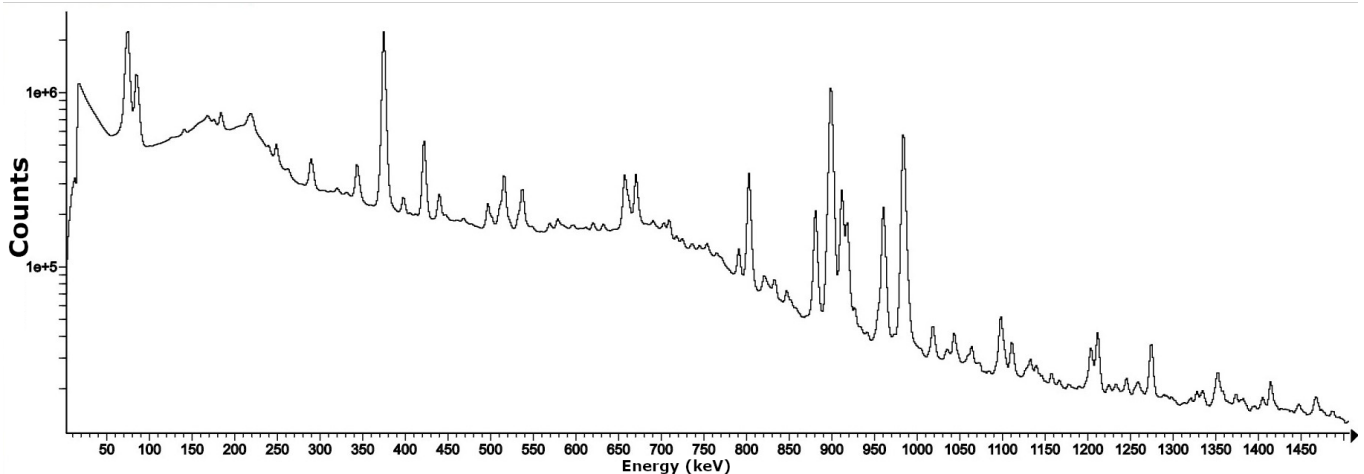


FIG. 1. γ spectrum from 0 - 1.5 MeV for the irradiation with protons of 30 MeV in a foil of natural lead. Data accumulated for 30 min and after 20 min of the irradiation.

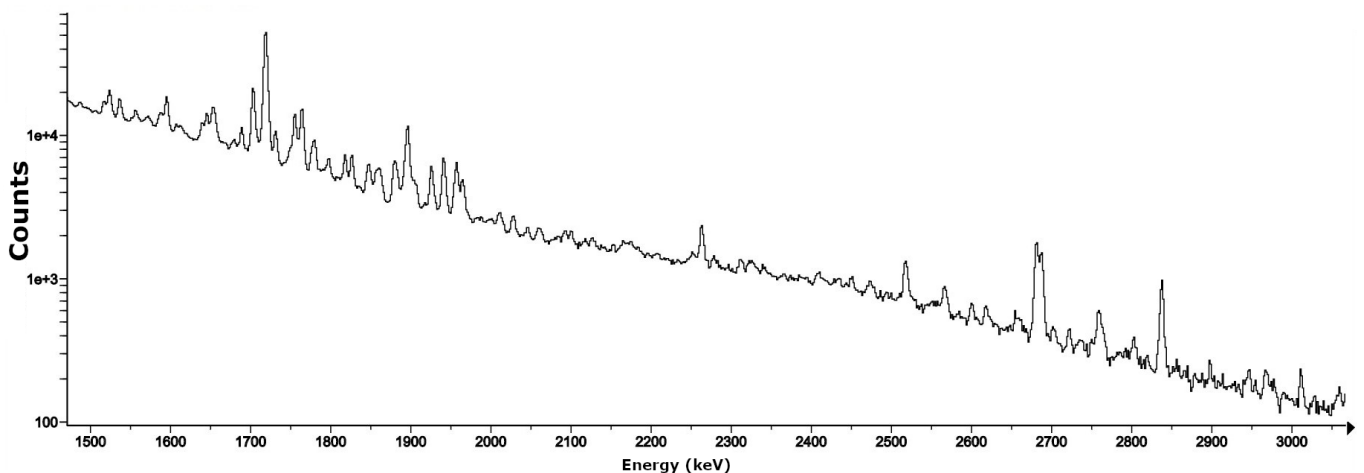


FIG. 2. γ spectrum from 1.5 - 3.0 MeV for the irradiation with protons of 30 MeV in a foil of natural lead. Data accumulated for 30 min and after 20 min of the irradiation.

We analyzed by gamma spectroscopy all lines with intensity greater than 1%, measuring the half-life of each

one in order to select the pure ones. For this analysis, we choose the spectrum produced by 18 MeV protons, since it is “cleaner”. Tables I and II summarize the γ intensities for $^{205,206}\text{Bi}$ EC decay deduced from our work in comparison with the previous works of Manthuruthil *et al.* [3] and Hamilton *et al.* [4] used as reference in Nuclear Data Sheets (ENDS), [5, 6]. Overall agreement between the previous results were obtained, although ours are generally more precise. The 895.12 keV (15.67%) from ^{206}Bi are overlapped by 894.56 keV (0.622%) from ^{205}Bi . We subtracted this contribution from the peak area using the previous works in ENDS. The discrepancy in our results in comparison with that of Manthuruthil *et al.* [3] may be due to subestimation of γ -intensity from the decay of ^{205}Bi . Other cases of overlapping are the 497.06 keV (15.33%; ^{206}Bi) with the 498.87 keV (0.040%; ^{205}Bi) and 498.40 keV (0.093%; ^{205}Bi). In the cases of γ intensities calculated for ^{205}Bi we observed an overlap in the 1903.45 keV (2.47%; ^{205}Bi) with the 1903.56 keV (0.349%) from ^{206}Bi . In all these cases the contribution of the “poison” gammas are much smaller and were corrected. On the other hand, the 570.60 keV (4.34%) from ^{205}Bi are overlapped by the 569.698 keV (97.75%) from ^{207}Bi (31.55 y). The uncertainty due to this correction is big enough, since ^{207}Bi is largely produced from $^{nat}\text{Pb}(p, xn)$ reactions at 18 MeV. For this reason we choose not to estimate this γ intensity.

We should also note the case of 987 keV. Although it is an overlapping of two γ 's from ^{205}Bi , almost all contribution comes from the 987.66 (16.1%). We could neglect that from 987.49 keV, since it has an intensity of 0.09%. The same happens with the 284 keV, since 284.15 keV (1.69%) is much more intense than that from 284.26 keV (0.031%).

Tables III and IV summarize the resulting cross-sections obtained in our work for the reaction $^{nat}\text{Pb}(p, xn)$. In Table V we summarize the cross-sections results for $^{206}\text{Pb}(p, 3n)^{204}\text{Bi}$ obtained in this work. In Table VI we summarize the cross-sections results for $^{204}\text{Pb}(p, xn)$ reactions. Since the neutron separation energy of the ^{205}Bi is 8.490 MeV, only $^{204}\text{Pb}(p, n)^{204}\text{Bi}$ reaction occurs for protons up to 24 MeV. As we can observe in Figure 3, after 25 MeV, the cross-section has a huge increase due to the contribution of $^{204}\text{Pb}(p, 3n)^{204}\text{Bi}$ reactions. Until 27 MeV, $^{204}\text{Pb}(p, n)$ still contributes. We can perform an extrapolation to subtract this reaction from the total one. After that, all the cross-section is due to $^{206}\text{Pb}(p, 3n)$ reactions. In the case of $^{201,202}\text{Bi}$, only $^{204}\text{Pb}(p, xn)$ reactions occur below 30 MeV.

In Figures 3, 4, 5, 6, 7, 8 and 9 we can observe the results for $^{nat}\text{Pb}(p, xn)$ obtained in this work in comparison with Talys 1.9 code simulations, [7], and previous works. While the previous ones have uncertainties of $\sim 10\%$, we increased the accuracy of the cross-sections by a factor > 5 (uncertainties $\sim 1-5\%$) due to long measurements and half-life curves fit. In the case of $^{nat}\text{Pb}(p, xn)^{207}\text{Bi}$, we have done the first measurement below 30 MeV for this reaction. Our results also reproduce the main features of

TABLE I. Gamma rays emitted in the decays of ^{206}Bi .

E_γ (keV)	I (This Work)	I (Previous Work) ^a
1878.65	0.01345 (28)	0.0203 (5)
1718.70	0.2413 (10)	0.322 (7)
1595.27	0.0410 (12)	0.0507 (11)
1405.01	0.0129 (10)	0.015 (4)
1098.26	0.1335 (10)	0.1365 (28)
1018.63	0.0786 (8)	0.0767 (16)
895.12	0.2044 (12) ^b	0.158 (3)
881.01	0.6859 (19)	0.669 (14)
803.10	1.0000 (24)	1.000 (20)
657.16	0.0188 (8)	0.0193 (5)
632.25	0.0427 (7)	0.0452 (10)
620.48	0.0531 (7)	0.0582 (12)
537.45	0.2679 (10)	0.308 (6)
516.18	0.3629 (12)	0.412 (8)
497.06	0.1323 (11) ^c	0.155 (3)
398.00	0.0873 (7)	0.1086 (22)
343.51	0.1942 (8)	0.237 (5)
262.70	0.0449 (5)	0.0305 (7)
183.977	0.1370 (7)	0.160 (4)

^a Manthuruthil *et al.* [3]; normalized.

^b 894.56 (5) keV (0.622(12)%, absolute intensity) contribution from ^{205}Bi EC decay was subtracted, Hamilton *et al.* [4].

^c 498.87 (20) (0.040(25)%, absolute intensity) and 498.40 (15) keV (0.093(16)%, absolute intensity) contributions from ^{205}Bi EC decay were subtracted, Hamilton *et al.* [4].

TABLE II. Gamma rays emitted in the decays of ^{205}Bi .

E_γ (keV)	I (This Work)	I (Previous Work) ^a
1903.45	0.0668 (3) ^b	0.0760 (22)
1861.70	0.1772 (5)	0.190 (6)
1775.80	0.1194 (4)	0.123 (4)
1764.30	1.0000 (16)	1.00 (3)
1619.10	0.01280 (27)	0.0113 (5)
1614.30	0.0771 (5)	0.0702 (22)
1551.00	0.0308 (6)	0.0298 (11)
1548.65	0.0104 (4)	0.0086 (5)
1351.52	0.0438 (5)	0.0326 (12)
1190.03	0.0931 (5)	0.0695 (26)
1043.75	0.3139 (8)	0.231 (6)
987.66+987.49 ^c	0.6929 (12)	0.498 (16)
910.90	0.0710 (4)	0.0505 (16)
761.35	0.0272 (3)	0.0209 (10)
759.10	0.0486 (4)	0.0320 (17)
703.45	1.2609 (18)	0.9569 ^d
579.80	0.2088 (5)	0.167 (5)
576.30	0.00645 (26)	0.00579 (25)
573.85	0.02380 (29)	0.0191 (6)
549.84	0.1057 (4)	0.0908 (25)
284.26+284.15 ^e	0.05626 (26)	0.0530 (15)
260.50	0.03652 (21)	0.0335 (12)

^a Hamilton *et al.* [4]; normalized.

^b 1903.56 (10) keV (0.349(15)%, absolute intensity) contribution from ^{206}Bi EC decay was subtracted, Manthuruthil *et al.* [3].

^c Main contribution comes from 987.66 keV (16.1(3)%, absolute intensity); 987.49 keV represents 0.09(3)% (absolute intensity), according to previous work.

^d No uncertainty estimated by this work.

^e Main contribution comes from 284.15 keV (1.69(3)%, absolute intensity); 284.26 keV represents 0.031(9)% (absolute intensity), according to previous work.

TABLE III. Cross-section values (mb) for proton energy in the lab frame for the reactions $^{nat}Pb(p, xn)^{204-207}Bi$.

Energy (MeV)	^{207}Bi	^{206}Bi	^{205}Bi	^{204}Bi
30.0	116.8 (19)	459 (5)	220 (6)	152 (7)
29.0	280.3 (25)	755 (11)	361 (16)	293 (42)
28.0	242 (4)	665 (7)	299 (12)	202 (10)
27.0	-	585 (6)	372 (11)	127 (6)
26.0	464 (8)	457 (5)	353 (11)	56.4 (29)
25.0	859 (14)	365 (3)	356 (10)	8.7 (4)
24.0	799 (14)	278.3 (28)	296 (9)	1.24 (7)
23.0	688 (6)	270.0 (27)	283 (8)	1.35 (7)
22.0	618 (6)	238.7 (24)	245 (7)	1.79 (9)
21.0	587 (5)	239.4 (24)	236 (7)	2.49 (13)
20.0	628 (6)	250.7 (25)	215 (6)	2.81 (15)

TABLE IV. Cross-section values (mb) for proton energy in the lab frame for the reactions $^{nat}Pb(p, xn)^{201-203}Bi$.

Energy (MeV)	^{203}Bi	^{202}Bi	^{201}Bi
30.0	4.53 (17)	4.89 (8)	0.349 (18)
29.0	8.9 (7)	10.72 (19)	-
28.0	10.0 (5)	5.25 (9)	-
27.0	12.2 (5)	2.38 (4)	-
26.0	13.2 (5)	0.510 (9)	-
25.0	14.1 (5)	-	-
24.0	12.8 (5)	-	-
23.0	12.3 (5)	-	-
22.0	11.0 (4)	-	-
21.0	8.5 (4)	-	-
20.0	7.5 (3)	-	-

the theoretical curve calculated by TALYS nuclear code. With exception of the $^{nat}Pb(p, 4n)^{201}Bi$ TALYS curve, all the others were translated right by 4 MeV. Due the big uncertainties, previous works were not able to verify fine discrepancies in theoretical curves. We will discuss more about this later.

The first measurement of the cross-section of $^{204}Pb(p, 4n)^{201}Bi$ reaction in the threshold energy is of special interest for nuclear reactions models. It has two intense high energy γ 's, the 1650.9 keV (6.3%) and the 1014.1 keV (11.6%). Since ^{204}Pb has an isotopic abundance of only 1.4% in comparison to 24.1% for the ^{206}Pb , and the cross-section for production of ^{204}Bi (11.22 h) on natural lead are about 400 times bigger than for the production of ^{201}Bi (103 min), the 1652.10 keV (24.1%) will lie in the same peak. This is due to the large width to have enough statistics of 1650.9 keV. In Figure 10 we can see the fit of this peak assuming these two γ 's. Statistically we can assert the presence of ^{201}Bi . The same holds for the 1014.1 keV, whose peak is merged with the 1014.30 keV of ^{205}Bi ($I_\gamma = 0.914\%$, 15.31 d), as can be seen in Figure 11. The 847.7 keV is an emblematic one. Its peak is a sum of four γ 's, from ^{201}Bi ($I_\gamma = 1.9\%$, 103 min), ^{201m}Bi ($I_\gamma = 100\%$, 57.5 min), ^{203}Bi ($I_\gamma = 8.6\%$, 11.76 h) and ^{204}Bi ($I_\gamma = 0.96\%$, 11.22h). As we can see in Figure 12, we can statistically assert the presence of ^{201}Bi . We did not use the 847 keV peak to calculate the

cross-section for $^{204}Pb(p, 4n)^{201}Bi$ for two main reasons: we did not know how much of the metastate was populated at 30 MeV and the uncertainty in this separation is big enough to have a reliable value for the cross-section.

Finally we report that some levels of ^{204m}Pb are probably fed by the decay of ^{204}Bi . Since we did not performed coincidence measurement, we cannot have a conclusive result. ^{204}Bi EC decay emits two 911 keV γ 's: 911.96 keV (11.22%), and 911.74 keV (13.6%). The 911.74 keV is emitted by the transition of the $2185.88 \mapsto 1274.13$ keV ($9^- \mapsto 4^+$). The 2185.88 keV level is a isomeric one with a half-life of 66.93 min. Although not report in nuclear databases, this γ represents a delayed one and it is important to consider in astrophysical models. When we follow the decay of ^{204}Bi by the 911 keV peak, we observe exactly this behavior, as noted in Figure 13. It is emitted by this transition and by another than feed the fundamental level of ^{204}Pb directly: $E_\gamma = 911.96$ keV ($3170.37 \mapsto 2258.15$ keV; $5^- \mapsto 5^-$). We note a similar behavior for the 532.72 keV γ , although it is not expected, Figure 14. If it only the gamma emitted by the $3638.05 \mapsto 3105.29$ keV γ -transition, it should not have a delay of ~ 60 min, as observed. Like in the 911 keV, it could have another transition from 2185.85 keV level (66.93 min). Since our measurements are in the statistical limit of compatibility for a delayed gamma emission, we recommend new measurements to establish the levels fed by ^{204}Bi .

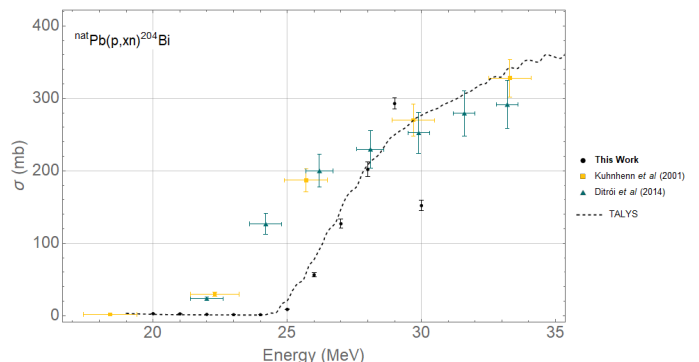


FIG. 3. Independent cross-sections for $^{nat}Pb(p, xn)^{204}Bi$ reactions, compared with earlier experimental data together with theoretical calculations from TALYS 1.9 default code. The experimental data are taken from Refs. [8, 9].

IV. DISCUSSION

Previous measurements of $^{nat}Pb(p, xn)^{201-207}Bi$ cross-sections at energies < 40 MeV by Kuhnhehn *et al.* [8], Ditri *et al.* [9], Lagunas-Solar *et al.* [10], Bell and Skarsgard [11] have discrepancies among each other of about a factor 2. Due the huge uncertainties of these works, they are compatible among each other, but do not allow to verify small variations in theoretical predictions for these cross-sections. By careful gamma spectroscopy

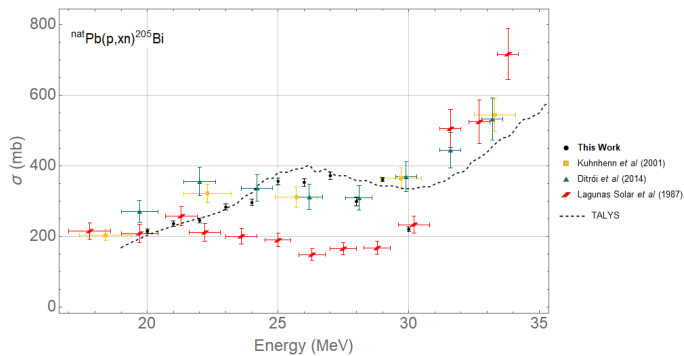


FIG. 4. Independent cross-sections for $^{nat}\text{Pb}(p,xn)^{205}\text{Bi}$ reactions, compared with earlier experimental data together with theoretical calculations from TALYS 1.9 default code. The experimental data are taken from Refs. [8–10].

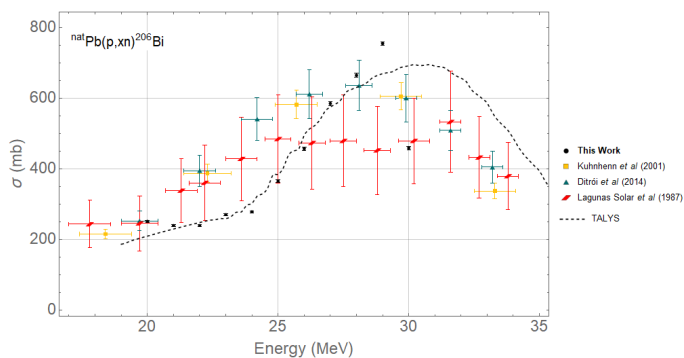


FIG. 5. Independent cross-sections for $^{nat}\text{Pb}(p,xn)^{206}\text{Bi}$ reactions, compared with earlier experimental data together with theoretical calculations from TALYS 1.9 default code. The experimental data are taken from Refs. [8–10].

with half-lives measurements, we were able to obtain high accuracy values for them and test TALYS code 1.9 simulations for (p,xn) reactions and TENDL-19 libraries, [12]. We noticed that these theoretical results overestimate (p,xn) cross-sections in general. When we shift TALYS curve by $\sim 4\text{ MeV}$, they reproduce the main experimental features. Since lead's isotopes are deformed nuclei, wrong estimation of the Coulomb barrier could lead to overestimated results too. Also, wrong neutron binding energy estimation could get the same discrepancies. Mokhtari Oranj *et al.* [13] compared several nuclear models for (p,xn) reactions on lead and possible combinations of the 24 nuclear input parameters to find the sensitivity of the cross sections to each nuclear model, mainly based on optical models potentials (OMP), nuclear level density (NLD) and γ -ray strength functions (γ SFs). At low energies, all models are pretty similar, but we note a shift of a few MeV among them. In general, JLM-Nolte α OMP-HCM-GHFB [14] and KD- α OMPIII-HFB-RMF [15], whose major alteration stems from the NLD parameters, have the best results. A linear combination of different models would result in a function that fit cross-sections at low and high

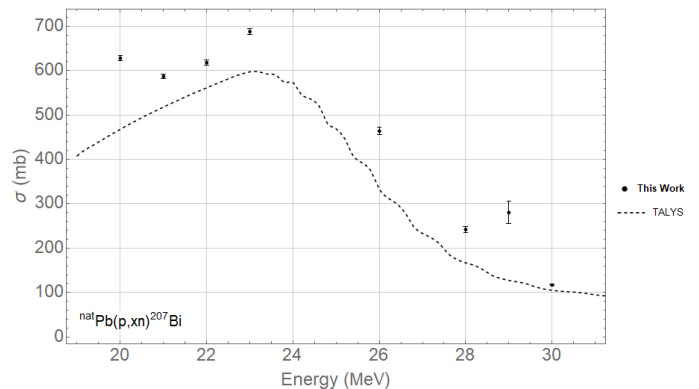


FIG. 6. Independent cross-sections for $^{nat}\text{Pb}(p,xn)^{207}\text{Bi}$ reactions, compared with theoretical calculations from TALYS 1.9 default code. There is no previous experimental data for this reaction.

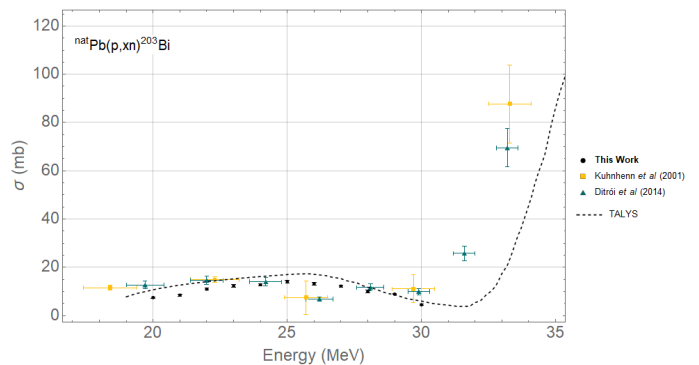


FIG. 7. Independent cross-sections for $^{nat}\text{Pb}(p,xn)^{203}\text{Bi}$ reactions, compared with earlier experimental data together with theoretical calculations from TALYS 1.9 default code. The experimental data are taken from Refs. [8, 9].

energies. Our results, allows us to test these models at a low energy range that was never done before.

We did the first measurement of the $^{nat}\text{Pb}(p,xn)^{207}\text{Bi}$ at energies below 40 MeV. Titarenko *et al.* [16] studied this reaction for energies between 40-2600 MeV. Schery *et al.* [17] did only one measurement of $^{208}\text{Pb}(p,n)^{208}\text{Bi}$ cross-section with $E_p = 25.8\text{ MeV}$. In general, $(p,2n)$ have higher cross-sections values for heavy elements at these energies, but $^{206-208}\text{Pb}$ contribute to the production of ^{208}Bi .

We also did the first measurement of the $^{204}\text{Pb}(p,4n)^{201}\text{Bi}$ cross-section at the threshold energy. The production of neutron deficient nucleus in the threshold is an important probe to test nuclear potentials of p-isotopes. This is of fundamental importance in astrophysical models for nucleosynthesis of heavy rp-elements, whose production in stars is still a subject of research. We note a good agreement between this result and TALYS simulations.

At 30 MeV, our results are depleted in comparison to TALYS simulations, when $(p,4n)$ reactions are allowed

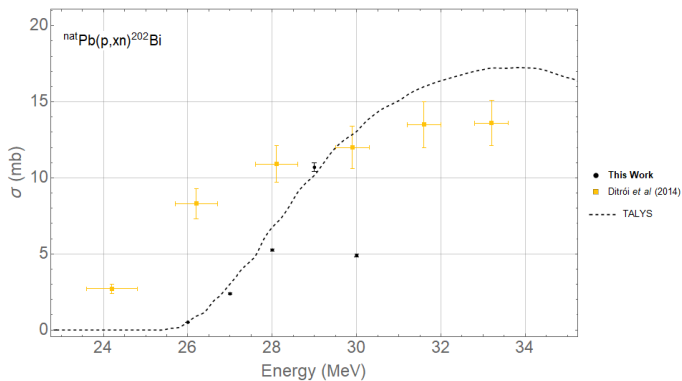


FIG. 8. Independent cross-sections for $^{nat}Pb(p, xn)^{202}Bi$ reactions, compared with earlier experimental data together with theoretical calculations from TALYS 1.9 default code. The experimental data are taken from Ref. [8].

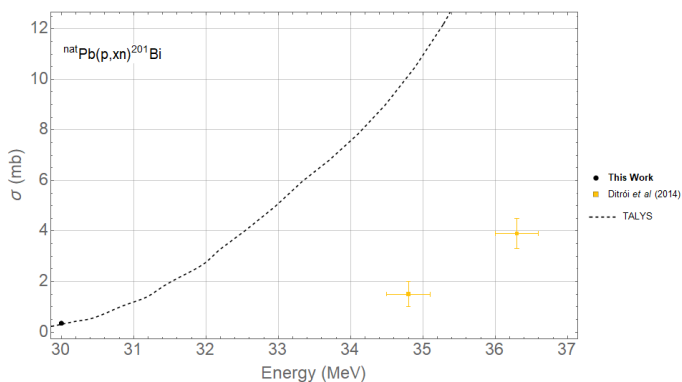


FIG. 9. Independent cross-sections for $^{nat}Pb(p, xn)^{201}Bi$ reactions, compared with earlier experimental data together with theoretical calculations from TALYS 1.9 default code. The experimental data are taken from Ref. [8].

to occur too. Since, for $^{204}Pb(p, 4n)^{201}Bi$ we got a good agreement without any shift of the theoretical curve, we think that only $(p, 1-3n)$ curves are being overestimated by TALYS. $^{nat}Pb(p, xn)$ is a sum of all possible curves involving lead isotopes, so, assuming that $(p, 4n)$ curve is better estimated by it, $^{nat}Pb(p, xn)$ with $E \geq 30$ MeV should have a lower value, as we measured.

The nuclear structure and decay of $^{201-205}Bi$ still needs a careful study. The γ -transitions of them were measured in works of more than 30 years and several transitions were marked as “probable”, although never studied again, [5, 6, 18–24]. We highlight here the case of ^{204}Pb . As expected, we observed that the 911.96 keV emitted from the decay of ^{204}Bi is due the decay of ^{204m}Pb and should be noted in NNDS. This has important implications in nucleosynthesis, since this γ is a delayed one and should be considered in dynamic models. It is also important in high performance liquid chromatography (HPLC) and time differential perturbed angular correlation (TDPAC) in macromolecules, [25]. The work of Cross [26] as adopted in Chiara and Kondev [27]

TABLE V. Cross-section values (mb) for proton energy in the lab frame for the reactions $^{206}Pb(p, xn)^{204}Bi$.

Energy (MeV)	^{204}Bi
30.0	631 (7)
29.0	1215 (42)
28.0	838 (10)
27.0	~ 516 (6)
26.0	~ 229.9 (29)
25.0	~ 32.0 (4)
24.0	-
23.0	-
22.0	-
21.0	-
20.0	-

TABLE VI. Cross-section values (mb) for proton energy in the lab frame for the reactions $^{204}Pb(p, xn)^{201-204}Bi$.

Energy (MeV)	^{204}Bi	^{203}Bi	^{202}Bi	^{201}Bi
30.0	-	323.57 (17)	349.29 (8)	24.929 (18)
29.0	-	635.7 (7)	765.71 (19)	-
28.0	-	714.3 (5)	375.00 (9)	-
27.0	-	871.4 (5)	170.04 (4)	-
26.0	-	942.9 (5)	36.42 (9)	-
25.0	-	1007.1 (5)	-	-
24.0	88.6 (7)	914.3 (5)	-	-
23.0	96.43 (7)	878.6 (5)	-	-
22.0	127.86 (9)	785.7 (4)	-	-
21.0	177.86 (13)	607.1 (4)	-	-
20.0	200.71 (15)	535.7 (3)	-	-

(NDS) measured first the γ 's and levels and then concluded that the 911.7 keV γ was compatible with IT level of ^{204m}Pb . It did not discuss that the intensity of this γ was measured immediately after EOB. Without that, it is not possible to have a precise γ intensity when mixing γ 's from ^{204}Pb and ^{204m}Pb , since their decay constants are different. Our work could not have a definite answer for this question, because we did not perform a coincidence gamma spectroscopy, although the fit of the 911 keV curve half-life did not support this. The 532.72 keV decay curve indicates that this level is possibly being fed by the ^{204m}Pb . There are some levels from the ^{204m}Pb (2185.88 keV, 9^-) whose level, spin and parity would allow a γ of 532 keV. Our result is in the limit of the confidence level, so we have not a strong evidence. Since the ^{204}Bi EC decay shows some discrepancies, we recommend a new measurement of the levels structure of this decay.

The new determination of γ -rays' intensities from $^{205,206}Bi$ agrees with previous results of Manthuruthil *et al.* [3] and Hamilton *et al.* [4], but it is in general more precise, due the measurements of decay curves, high precision gamma spectroscopy and data analysis, although some discrepancies have been found. In some cases, we considered these previous studies to subtract negligible γ 's contamination. This iterative approach, although unusual, when comparing with anti-Compton and coincidence approaches should lead in an error of $\ll 5\%$, depending on the accuracy of these results. This way

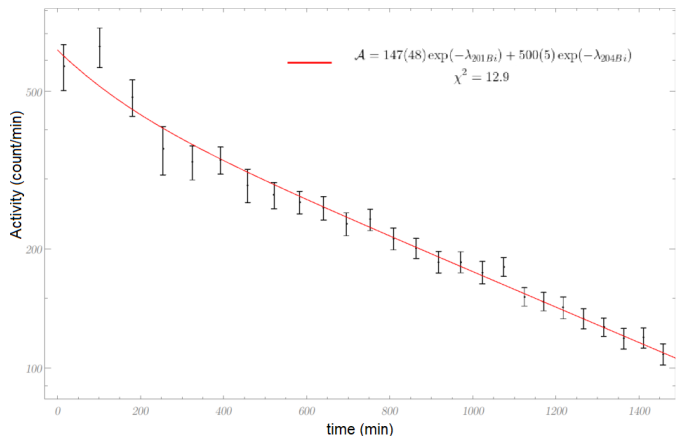


FIG. 10. Activity decay curve (counts/min) for $E_\gamma = 1650.9 \text{ keV}$ from ^{201}Bi (6.3%, 103 min) with $E_\gamma = 1652.10 \text{ keV}$ from ^{204}Bi (0.56%, 11.22 h), obtained from irradiation of natural lead with protons of 30 MeV.

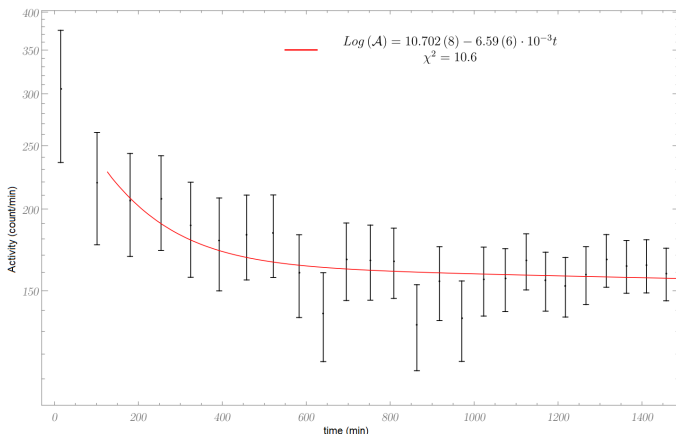


FIG. 11. Activity decay curve (counts/min) for $E_\gamma = 1014.1 \text{ keV}$ from ^{201}Bi (11.6%, 103 min) with $E_\gamma = 1014.3 \text{ keV}$ from ^{205}Bi (0.941%, 15.31 d), obtained from irradiation of natural lead with protons of 30 MeV.

opens the possibility of high precision spectroscopy and data analysis (HPSDA) in substitution to more complex experimental arrangements, that should always be considered, whenever possible.

The study of (p, xn) reactions in heavy elements, specially in neutron-deficient isotopes with protons of $E_p < 50 \text{ MeV}$ could represent a possible path for the rp/r -process, acting together in a dynamic production called r^2p -process, as proposed by Guillaumon and Goldman [28]. The high energy protons could be produced by bubbles and jets in neutrino-driven winds from neutron stars mergers and supernovae with $T \geq 3 \times 10^9 \text{ K}$, followed by a “freeze-out”, [29–34]. Together with the α -process proposed by Woosley and Hoffman [29], this could produce all the rp/r -elements, including heavy rp -elements and thorium and uranium, whose nucleosynthesis is not still completely understood. Due that, ex-

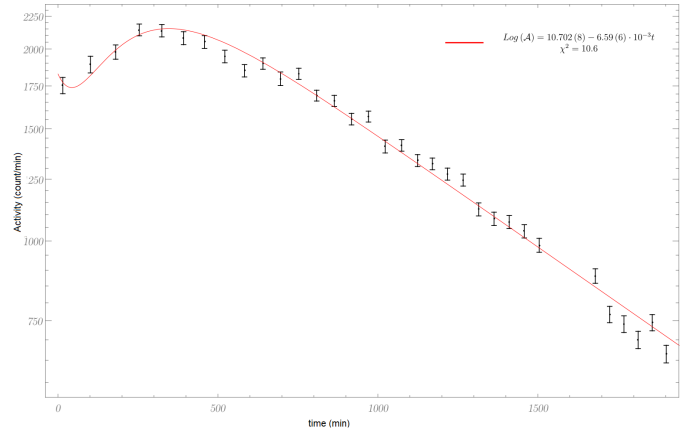


FIG. 12. Activity decay curve (counts/min) for $E_\gamma = 1014 \text{ keV}$ from ^{201}Bi (1.9%, 103 min), ^{201m}Bi (100%, 57.5 min), ^{201m}Bi (8.6%, 11.76 h), and ^{204}Bi (0.96%, 11.22 h) obtained from irradiation of natural lead with protons of 30 MeV. We could not estimate the percentage of ^{201m}Bi that is populated in this reaction.

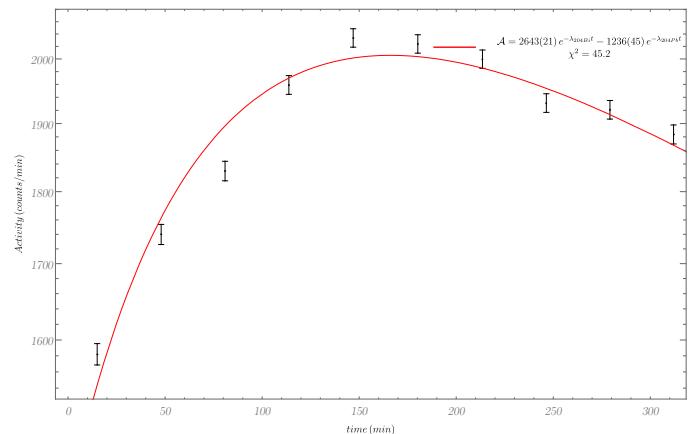


FIG. 13. Activity decay curve (counts/min) for $E_\gamma = 911.96 \text{ keV}$ (11.2%) and 911.74 keV (13.6%) from ^{204}Bi . The last one comes from the γ -transition of ^{204m}Pb (91.5%, 66.93 min), as can be seen from our fit. This delayed γ was not completely reported at ENDS.

perimental (p, xn) cross sections in heavy elements and neutron-deficient isotopes are of special importance in nucleosynthesis models.

V. CONCLUSIONS

We were able to determine the cross-sections for $^{nat}\text{Pb}(p, xn)^{201-207}\text{Bi}$, $^{204}\text{Pb}(p, xn)^{201-204}\text{Bi}$ and $^{206}\text{Pb}(p, xn)^{204}\text{Bi}$ reactions in the range 20 – 30 MeV. Previous works have big discrepancies among each other, although statistically compatible due the big uncertainties. Our results increase dramatically the accuracy of these cross-sections, allowing us to compare with TALYS code and TENDL curves. For (p, γ) and $(p, 1-3n)$ curves,

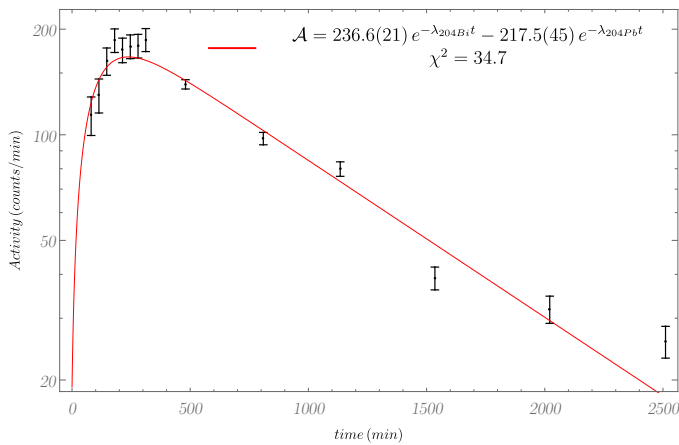


FIG. 14. Activity decay curve (counts/min) for $E_\gamma = 532.72 \text{ keV}$ from ^{204}Bi (1.36%). This fit indicates this transition is possibly fed by the ^{204m}Pb (66.93 min), although statistically not conclusive.

we needed to shift the curves for about 4 MeV, probably to wrong theoretical estimation of neutron binding energy and deformed Coulomb barrier. We did the first measurement of $^{204}\text{Pb}(p, xn)^{201}\text{Bi}$ in the threshold and of $^{nat}\text{Pb}(p, xn)^{207}\text{Bi}$. Reactions with protons in the threshold for neutron deficient isotopes are an important probe of nuclear potentials in the β^+ region and will affect nucleosynthesis models for the rp-elements.

We also obtained more precise results for γ intensities of $^{205,206}\text{Bi}$. Our results are in good agreement with previous ones.

The nuclear structure of stable lead isotopes need a reevaluation, since there are still possible transitions that were never confirmed. In the case of ^{204}Bi decay, we report that the γ of 911.77 keV feed the ^{204m}Pb (66.93 min), representing a delayed γ and should be update in Nuclear Data Sheets. We also show indicatives that the 532 keV could being fed by the ^{204m}Pb , although a conclusive study should be made.

-
- [1] P. V. Guillaumon, *Study of reactions $^{nat}\text{Pb}(p, xn)^{201-207}\text{Bi}$ and possible implications for the r-process*, Ph.D. thesis, Universidade de Sao Paulo (2019).
- [2] P. Gouffon, *Manual do programa IDEFIX* (Instituto de Física da Universidade de So Paulo, Laboratrio do Acelerador Linear, So Paulo, 1987).
- [3] J. C. Manthuruthil, D. C. Camp, A. V. Ramayya, J. H. Hamilton, J. J. Pinajian, and J. W. Doornebos, *Phys. Rev. C* **6**, 1870 (1972).
- [4] J. H. Hamilton, V. Ananthakrishnan, A. V. Ramayya, W. M. LaCasse, D. C. Camp, J. J. Pinajian, L. H. Kern, and J. C. Manthuruthil, *Phys. Rev. C* **6**, 1265 (1972).
- [5] F. Kondev, *Nuclear Data Sheets* **101**, 521 (2004).
- [6] F. Kondev, *Nuclear Data Sheets* **109**, 1527 (2008).
- [7] A. Koning and D. Rochman, *Nuclear Data Sheets* **113**, 2841 (2012), special Issue on Nuclear Reaction Data.
- [8] J. Kuhnenn, U. Herpers, W. Glasser, R. Michel, P. W. Kubik, and M. Suter, *Radiochimica Acta* **89**, 697 (2001).
- [9] F. Ditri, F. Trknyi, S. Takcs, and A. Hermanne, *Applied Radiation and Isotopes* **90**, 208 (2014).
- [10] M. C. Lagunas-Solar, O. F. Carvacho, L. Nagahara, A. Mishra, and N. J. Parks, *Int. J. Radiat. Appl. Instrum. Part A* **38**, 129 (1987).
- [11] R. E. Bell and H. M. Skarsgard, *Canadian Journal of Physics* **34**, 745 (1956), <https://doi.org/10.1139/p56-086>.
- [12] A. Koning, D. Rochman, J.-C. Sublet, N. Dzysiuk, M. Fleming, and S. van der Marck, *Nuclear Data Sheets* **155**, 1 (2019), special Issue on Nuclear Reaction Data.
- [13] L. Mokhtari Oranj, N. S. Jung, M. Bakhtiari, A. Lee, and H. S. Lee, *Physical Review C* **95**, 044609 (2017).
- [14] M. Nolte, H. Machner, and J. Bojowald, *Phys. Rev. C* **36**, 1312 (1987).
- [15] A. Koning and J. Delaroche, *Nuclear Physics A* **713**, 231 (2003).
- [16] Y. E. Titarenko, V. F. Batyaev, V. M. Zhivun, R. D. Mulambetov, S. V. Mulambetova, S. L. Zaitsev, S. G. Mashnik, and R. E. Prael, *AIP Conference Proceedings* **769**, 1070 (2005), <https://aip.scitation.org/doi/pdf/10.1063/1.1945192>.
- [17] S. Schery, D. Lind, H. Fielding, and C. Zafiratos, *Nuclear Physics A* **234**, 109 (1974).
- [18] H. Richel, G. Albouy, G. Auger, J. David, J. Lagrange, M. Pautrat, C. Roulet, H. Sergolle, and J. Vanhorenbeeck, *Nuclear Physics A* **267**, 253 (1976).
- [19] H. Richel, G. Albouy, G. Auger, F. Hanappe, J. Lagrange, M. Pautrat, C. Roulet, H. Sergolle, and J. Vanhorenbeeck, *Nuclear Physics A* **303**, 483 (1978).
- [20] B. S. Dzhelepov, M. Y. Kuznetsova, T. I. Popova, and V. P. Prikhodtseva, *Izv. Akad. Nauk SSSR, Ser. Fiz.* **49**, 2082 (1985).
- [21] S. Goring and A. Hanser, *Z. Phys.* **271**, 183 (1974).
- [22] F. Kondev, *Nuclear Data Sheets* **108**, 365 (2007).
- [23] F. Kondev, *Nuclear Data Sheets* **105**, 1 (2005).
- [24] S. Zhu and F. Kondev, *Nuclear Data Sheets* **109**, 699 (2008).
- [25] S. Friedemann, F. Heinrich, H. Haas, and W. Trger, *Hyperfine Interactions* **159**, 313 (2004).
- [26] J. B. Cross, *The Electron Capture Decay Schemes of Bi^{203} and Bi^{204}* , Ph.D. thesis, Michigan State Univ. (1970).
- [27] C. Chiara and F. Kondev, *Nucl. Data Sheets* **111**, 141 (2010).
- [28] P. V. Guillaumon and I. D. Goldman, “The importance of charged particle reactions in the r-process on supernovae and neutron stars,” (2020), arXiv:2009.01814 [nucl-th].
- [29] S. E. Woosley and R. D. Hoffman, *Astrophys. J.* **395**, 202 (1992).
- [30] A. G. W. Cameron, *The Astrophysical Journal* **587**, 327 (2010).
- [31] J. Bliss, A. Arcones, F. Montes, and J. Pereira, *Journal of Physics G Nuclear Physics* **44**, 054003 (2017), arXiv:1612.02435 [astro-ph.SR].
- [32] W. M. Howard, S. Goriely, M. Rayet, and M. Arnould, *Astrophys. J.* **417**, 713 (1993).
- [33] A. Arcones and G. Martínez-Pinedo, *Phys. Rev. C* **83**,

- 045809 (2011).
- [34] A. Perego, S. Rosswog, R. M. Cabezn, O. Kobkin, R. Kppeli, A. Arcones, and M. Liebendrfer, *Monthly Notices of the Royal Astronomical Society* **443**, 3134 (2014), <https://academic.oup.com/mnras/article-pdf/443/4/3134/6276168/stu1352.pdf>.